Food Chemistry 392 (2022) 133257

Contents lists available at ScienceDirect

Food Chemistry

journal homepage: www.elsevier.com/locate/foodchem

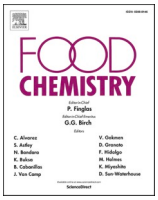

Influence of emulsifier type and encapsulating agent on the *in vitro* digestion of fish oil-loaded microcapsules produced by spray-drying

Nor E. Rahmani-Manglano [1], Manuel Tirado-Delgado [1], Pedro J. García-Moreno [*], Antonio Guadix, Emilia M. Guadix

Department of Chemical Engineering, University of Granada, Granada, Spain

ARTICLE INFO

Keywords:
Omega-3 polyunsaturated fatty acids
Microencapsulation
Whey protein concentrate hydrolysate
Interfacial composition
INFOGEST protocol
Lipolysis

ABSTRACT

The influence of the emulsifier type and the encapsulating agent on the bioaccessibility of microencapsulated fish oil was investigated. Fish oil-loaded microcapsules were produced by spray-drying using carbohydrate-based encapsulating agents (glucose syrup or maltodextrin). Whey protein concentrate hydrolysate (WPCH) or Tween 20 (TW20) were used as the emulsifiers. The microcapsules were subjected to a three-phase *in vitro* digestion (oral, gastric, and intestinal phase) and the changes in the physicochemical properties of the samples were monitored throughout the simulated gastrointestinal tract (oil droplet size, ζ-potential, and microstructure). The lipolysis rate and extent were evaluated at the intestinal digestion phase. Contrary to the encapsulating agent, the emulsifier used in the infeed emulsion formulation significantly influenced lipid digestion. WPCH-based interfacial layer prevented oil droplets coalescence during and after processing more efficiently than TW20, which resulted in an increased specific surface area for lipases to adsorb and thus a higher bioaccessibility of the microencapsulated oil.

1. Introduction

Fish oil is an important source of long chain omega-3 polyunsaturated fatty acids (PUFAs) such as eicosapentaenoic acid (C20:5n-3, EPA), and docosahexaenoic acid (C22:6n-3, DHA) (Calder & Yaqoob, 2009). These PUFAs have been recognized to play an important role in human health by, for instance, diminishing the risk of cardiovascular disease, hypertension, or cancer (Punia et al., 2019). However, the low intake of omega-3 PUFAs through the diet makes it necessary to enrich common foods with these bioactive lipids to ensure their daily intake (Jacobsen et al., 2013). Nonetheless, EPA and DHA are highly prone to oxidation, which requires the development of delivery systems for their successful inclusion into complex food matrices (Rahmani-Manglano et al., 2020a).

Microencapsulation by spray-drying is the most commonly used technique in the food industry to protect easily-degradable bioactive compounds before food enrichment (Champagne & Fustier, 2007). In the case of omega-3 PUFAs rich oils (e.g., fish oil), the process involves the emulsification of the hydrophobic phase within the wall constituents, which generally consist of an aqueous solution containing the encapsulating agent and, depending on its surface-active properties, an emulsifier. Then, the infeed emulsion is atomized in the drying chamber into a hot air stream (150–200 °C) to evaporate the solvent and produce the dried microcapsules (Rahmani-Manglano et al., 2020a). Whilst the main aim of research in the field of fish oil microencapsulation has been monitoring the oxidative stability of omega-3 PUFAs during storage and subsequent inclusion into food matrices (Encina et al., 2016), recent trends in this field include the interest in understanding the digestion of these bioactive lipids throughout the gastrointestinal tract (GIT) (El-Messery et al., 2020; Shen et al., 2011; Solomando, Antequera, & Perez-Palacios, 2020a; Solomando, Antequera, & Perez-Palacios, 2020b). When microcapsules are ingested, they are exposed to fluids and enzymes present in the GIT which causes physicochemical changes. The bioaccessibility of the omega-3 PUFAs might vary depending on the components used to produce the microcapsules (Acevedo-Fani et al., 2021). Therefore, bioaccessibility can be improved by the efficient design of microcapsules using different combinations of emulsifiers and/or encapsulating agents.

Glucose syrup (GS) and maltodextrin (MD) are two commonly used encapsulating agents in spray-drying processing (Rahmani-Manglano

* Corresponding author.
E-mail address: pjgarcia@ugr.es (P.J. García-Moreno).
[1] Nor E. Rahmani-Manglano and Manuel Tirado-Delgado contributed equally to this work.

https://doi.org/10.1016/j.foodchem.2022.133257
Received 20 December 2021; Received in revised form 27 April 2022; Accepted 17 May 2022
Available online 20 May 2022

et al., 2020a). Polysaccharides can affect lipid digestion through different mechanisms such as adhering to the surface of oil droplets impeding lipase adsorption or increasing the viscosity of the continuous phase limiting the free flow of the digestive components, among others (Chang & McClements, 2016). The emulsifier used in the formulation of the infeed emulsion also has a great impact on lipid digestion due to its influence on oil droplets aggregation, avoiding or promoting oil droplets coalescence (McClements, 2018; Solomando, Antequera, & Perez-Palacios, 2020a). Besides, highly surface-active emulsifiers may prevent bile salts and lipase adsorption onto the lipid droplets surfaces, thus limiting lipolysis (McClements, 2018).

The bioaccessibility of microencapsulated marine oils (e.g., fish oil or krill oil) within protein, carbohydrate or protein/carbohydrate-based matrices produced by spray-drying has been recently investigated as the delivery system itself (Chang & Nickerson, 2018; El-Messery et al., 2020; Sánchez et al., 2021; Zhu et al., 2021) or incorporated into different food matrices (Shen et al., 2011; Solomando, Antequera, & Perez-Palacios, 2020a; Solomando, Antequera, & Pérez-Palacios, 2020b). However, the influence of the infeed emulsion formulation and processing on both, the physicochemical changes of the microcapsules within the simulated GIT and on the extent of the microencapsulated oil digestion has not been yet studied.

Recently, whey protein concentrate hydrolysate (WPCH) has been reported to be an excellent emulsifier for the stabilization of fish oil-in-water emulsions while also exerting antioxidant activity, thus enhancing its oxidative stability (Padial-Domínguez et al., 2020a). Furthermore, WPCH-stabilized fish oil-in-water emulsions containing carbohydrates as encapsulating agents have been successfully spray-dried to produce oxidatively stable fish oil-loaded microcapsules to be used as omega-3 delivery systems in the production of fortified low-fat mayonnaise (Rahmani-Manglano et al., 2020b). However, to the best of the authors' knowledge, the influence of WPCH, used as an emulsifier in the production of dried omega-3 PUFAs delivery systems, on lipid digestion has not been yet investigated.

Therefore, the aim of the study was to evaluate the effect of WPCH as an emulsifier on the bioaccessibility of microencapsulated fish oil produced by spray-drying when using GS or MD as encapsulating agents. The performance of WPCH was compared with a synthetic surfactant widely used by the food industry as Tween 20 (TW20). The INFOGEST standardized protocol for static *in vitro* digestion was employed to simulate digestion and the physicochemical changes of the dispersed microcapsules (i.e., microstructure, droplet size, ζ-potential) throughout the different phases of the simulated GIT, as well as the lipolysis rate and extent on the intestinal phase of *in vitro* digestion, were evaluated.

2. Materials and methods

2.1. Materials

Refined fish oil (Omega Oil 1812 TG Gold) was obtained from BASF Personal Care and Nutrition GmbH (Illertissen, Germany) and stored at −80 °C until use. Glucose syrup (GS; DE38, C*Dry 1934) was kindly provided by Cargill Germany GmbH (Krefeld, Germany). Maltodextrin (MD; DE21) and whey protein (ca. 35 wt% protein content) were generously donated by Abbott (Granada, Spain). Tween 20 (TW20) was purchased from Sigma-Aldrich (Darmstadt, Germany). Alcalase was purchased from Novozymes (Denmark).

For the simulated digestion process, α-amylase (from *Bacillus licheniformis* 500–1500 units per mg protein, A4551), pepsin from porcine gastric mucosa (>2500 units per mg protein, P7012), bile extract (from porcine, B8631), pancreatin from porcine pancreas (8 × USP specifications, P7545), and lipase from porcine pancreas (30–90 units per mg protein using triacetin, L3126) were purchased from Sigma-Aldrich (USA). The different salts used for the simulated digestion fluids, KCl, KH_2PO_4, NaCl, $MgCl_2(H_2O)_6$, $(NH_4)_2CO_3$, HCl, and $CaCl_2(H_2O)_2$ were bought either from Sigma-Aldrich (USA) or Merck (Germany). Nile red (Sigma-Aldrich S.A., USA) was used for the confocal microscopy. Enzyme activity analyses were performed according to the protocols described in (Brodkorb et al., 2019; Minekus et al., 2014).

2.2. Production of whey protein concentrate hydrolysate (WPCH)

The enzymatic hydrolysis of whey protein concentrate was carried out in an automatic titrator (718 Stat Titrino; Metrohm AG, Herisau, Switzerland) to a degree of hydrolysis of 10% (DH10) with alcalase, as described by Rahmani-Manglano et al. (2020b). The whey protein concentrate hydrolysate (WPCH) was freeze-dried and stored at 4 °C until further use.

2.3. Production of the microcapsules

Four types of microcapsules were produced depending on the encapsulating agent (i.e., GS or MD) and the emulsifier (i.e., WPCH or TW20) used in the infeed emulsion formulation. The emulsions prepared with WPCH as an emulsifier (ca. 6 wt%) had a final protein content of 2 wt%. The concentration of TW20 in the feed emulsion (0.35 wt%) was optimized to achieve a similar oil droplet size distribution compared to that of the WPCH-based emulsions. The total solids content of the emulsions was fixed to 39 wt% and depending on the emulsifier used, the concentration of the encapsulating agent varied as follows: 28 wt% when using WPCH or 34 wt% when using TW20 as emulsifiers. The aqueous phase of the emulsions was prepared by dissolving the encapsulating agent and the emulsifier in distilled water and stirring (500 rpm) overnight at room temperature. A pre-emulsion was prepared by dispersing the oil (5 wt%) in the aqueous phase for 2 min at 15,000 rpm using an Ultraturrax T-25 homogenizer (IKA, Staufen, Germany). The oil was added during the first minute. Afterwards, the coarse emulsion was homogenized in a high-pressure homogenizer (PandaPLUS 2000; GEA Niro Soavi, Lübeck, Germany) at a pressure range of 450/75 bar, applying 3 passes. The drying process was carried out in a laboratory-scale spray-drier (Büchi B-190; Büchi Labortechnik, Flawill, Switzerland) at 180/90 °C inlet/outlet temperature, respectively. The drying air flow was fixed to 25 Nm^3/h. The water content of the microcapsules obtained was lower than 5% when determined using an infrared balance (AD 471A, Tokyo, Japan).

2.4. Characterization of the microcapsules

2.4.1. Morphology and size

The morphology and size of the microcapsules were investigated by means of scanning electron microscopy (SEM) using a FESEM microscope (LEO 1500 GEMINI, Zeiss, Germany). A thin layer of microcapsules was placed on carbon tape and carbon-coated using an EMITECH K975X Turbo-Pumped Thermal Evaporator (Quorum Technologies, UK). The SEM images were acquired in the range 500X – 2KX magnification with a 5-kV accelerating voltage. The images were then analyzed using the ImageJ software (National Institute of Health) and>150 randomly-selected microcapsules were measured to determine the particle size distributions and mean diameters.

2.4.2. Encapsulation efficiency and surface fat

The encapsulation efficiency (EE) and the surface fat content (SF) were measured as described in our previous work (Rahmani-Manglano et al., 2020b). Approximately, 2.5 g of microcapsules were immersed in 15 mL of hexane and mixed for 2 min in a vortex mixer. Then, the mixture was centrifuged at 2720g for 20 min and 5 mL of supernatant were collected in a Pyrex tube previously weighted. Then, the hexane was evaporated under a constant flow of nitrogen and the amount of extracted oil was weighed. The oil concentration was adjusted to the original volume of hexane added. The EE and the SF were calculated as follows:

$$EE, \% = \frac{A - B}{A} \cdot 100 \quad (1)$$

$$SF, \% = \frac{B}{A} \cdot 100 \quad (2)$$

where A refers to the experimental total amount of oil (g) and B to the extractable oil (g). The experimental total oil load of the microcapsules was determined by extracting the fish oil using hexane:2-propanol (1:1, v/v) solvent. For the extraction, ca. 50 mg of powder was dissolved by adding 10 mL of distilled water. The experimental total oil load was determined by measuring the absorbance of the lipid extract at 250 nm in a UV–Vis double beam spectrophotometer (Thermo Spectronic Helios Alpha 9423 UVA 1002E, Thermo Fisher Scientific, USA). The amount of oil contained in the lipid phase was determined from a calibration curve ($R^2 = 0.99$) prepared by dissolving various quantities of fish oil in hexane (0.1 – 2.0 mg/mL). Measurements were carried out in triplicate.

2.5. Static in vitro digestion

The simulated digestion of the samples was carried out using an adaptation of the INFOGEST *in vitro* digestion method described by Brodkorb et al. (2019). The latter consists in a 3-phase digestion (i.e., mouth, stomach, small intestine) coupled with the pH-Stat method to assess the degree of hydrolysis of the fish oil (Chang & McClements, 2016). Blanks were made with either water or WPCH to evaluate the impact of the non-fatty components of the digestion on the results shown by the pH-Stat method. *In vitro* simulated digestions were carried out in triplicates.

2.5.1. Simulated digestion fluids

Simulated salivary fluid (SSF), simulated gastric fluid (SGF), and simulated intestinal fluid (SIF) were produced as described by Brodkorb et al. (2019) with some modifications. Since the pH-Stat method was used during the intestinal phase of digestion, $NaHCO_3$ was replaced by NaCl at the same molar ratio to avoid the formation of bubbles and changes in the pH, as previously reported by other authors (Mat et al., 2016; Yang & Ciftci, 2020).

2.5.2. Oral digestion

Briefly, 7.5 g of microcapsules were mixed with 7.5 mL of SSF preheated at 37 °C and the pH was set to 7 with NaOH 0.5 M. Subsequently, α-amylase (from *Bacillus licheniformis*) was added to reach an activity of 75 U/mL and the mixture was introduced in a shaker instrument (Heidolph Unimax 1010) at 37 °C and 250 rpm for 2 min.

2.5.3. Gastric digestion

Gastric lipolysis only represents between 10 and 30% of the total lipolysis (Favé et al., 2004) and, although the optimum pH for gastric rabbit lipase is pH 4 (Moreau et al., 1988), the INFOGEST protocol uses pH 3 for this stage (Brodkorb et al., 2019; Minekus et al., 2014) which could even diminish more the lipolysis extent in the gastric phase. Therefore, gastric rabbit lipase was omitted in this study. To continue with the procedure, 17.5 mL of SGF preheated at 37 °C were added to the result of the oral phase and the pH was set to 3 using HCl 1 N. Pepsin was added to reach an activity of 2000 U/mL in the final mixture, which was then introduced in the shaker at 37 °C and 250 rpm for 2 h.

2.5.4. Intestinal digestion with the pH-Stat method

Porcine bile extract to achieve a 10 mM of bile salts in the final mixture was diluted in 40 mL of SIF and heated in the shaker at 37 °C and 250 rpm for at least 30 min before the intestinal phase of *in vitro* digestion. The mixture obtained from the gastric digestion and the mixture of SIF and bile salts was poured into a jacketed beaker maintained at 37 °C. The pH of the mixture was adjusted to 7 with NaOH 1 N and pancreatin and pancreatic lipase were added to achieve 100 U/mL of trypsin activity and 2000 U/mL of lipase activity, respectively. The reaction was controlled at pH 7 for 2 h with a titrating instrument (902 Titrando, Metrohm, Herisau, Switzerland) by adding NaOH 0.2 M.

2.5.5. Determination of the percentage of free fatty acids

The percentage of free fatty acids (%FFA) was related to the volume of NaOH (0.2 M) added during the intestinal phase of *in vitro* digestion using the following equation (Yan Li & McClements, 2010):

$$\%FFA = 100 \cdot (VOil - VBlank) \cdot mNaOH \cdot \frac{MLipid}{2 \cdot WLipid} \quad (3)$$

where VOil (mL) represents the volume of NaOH added to neutralize the FFAs liberated, VBlank (mL) is the volume of NaOH added to neutralize the acid groups created by the components of the blanks, mNaOH is the molarity of the sodium hydroxide solution (0.2 M), MLipid is the molecular weight of the fish oil (930 g/mol) and WLipid is the total weight of lipid introduced in the reaction vessel (0.96 g).

2.6. Physicochemical changes during digestion

To study the fate of the microcapsules as they passed through the GIT, samples were taken from the end of the oral phase of the simulated digestion (Oral phase), as well as from the start and the end of the gastric and intestinal phases of *in vitro* digestion (Gastric/Intestinal phase 1 and Gastric/Intestinal phase 2, respectively). The parent emulsions before spray-drying were also characterized to evaluate the impact of processing on the reconstituted emulsions.

2.6.1. Oil droplet size

The oil droplet size distribution and oil droplet size of the samples was determined using a static light scattering instrument (Mastersizer 3000, Malvern Instruments, Worcestershire, United Kingdom). Samples were diluted in recirculating water (3000 rpm) to achieve an obscuration in the range 12–15%. The refractive indexes of fish oil (1.481) and water (1.330) were used as particle and dispersant, respectively. Measurements were made in triplicate.

2.6.2. Zeta potential

The ζ-potential of the samples was measured using a Zetasizer Ultra (Malvern Instruments Ltd., Worcestershire, UK) at 25 °C. Samples were previously diluted in a volume proportion of 2/1000 with distilled water at the pH of the respective GIT phase (pH 3 or pH 7), adjusted with either HCl (1 M) or NaOH (1 M). Measurements were made in triplicate.

2.7. Microstructure of the emulsion

For better understanding the microstructure of the systems studied, samples from the end of the oral phase and the end of the intestinal phase of *in vitro* digestion were stained with Nile Red to be observed using a confocal scanning laser microscopy instrument (Leica DMI6000 B, Germany). Staining was carried out by mixing 2 mL of the samples with 0.1 mL of a Nile Red solution (1 mg/mL in ethanol). To capture the images, a 60 × oil immersion objective lens was used with x3 zoom. The images were recorded with the software Leica Microsystems, establishing the spectrums of Nile Red in 543 nm for excitation and 650 nm for emission.

2.8. Statistical analysis

Data were subjected to analysis of variance (ANOVA) by using Statgraphics version 5.1 (Statistical Graphics Corp., Rockville, MD, USA). Tukeýs multiple range test was used to determine significant differences between mean values. Differences between mean values were considered significant at a level of confidence of 95% ($p \leq 0.05$).

3. Results and discussion

3.1. Characterization of the microcapsules

3.1.1. Morphology and size

All the microcapsules showed a spherical shape with both, smooth and wrinkled surfaces (Fig. 1A-D). Moreover, no particle agglomeration was observed. Overall, the encapsulating agent and the emulsifier used had little effect on the particle size since no significant differences in the mean diameter nor in the particle size distribution of the microcapsules was observed ($p > 0.05$) (Fig. 2A). The microcapsules mean diameter varied from 9.37 ± 5.20 μm to 10.54 ± 5.26 μm, and approximately 90% of the particles had a size below 20 μm for all the samples (Fig. 2A).

3.1.2. Encapsulation efficiency and surface fat

High EE was achieved in the four systems studied (>87%). However, significant differences ($p < 0.05$) were observed depending on the emulsifier used in the formulation (Fig. 2B). Irrespective of the encapsulating agent, WPCH-based microcapsules showed higher EE and thus lower SF than the TW20-based microcapsules counterparts. EE is largely dependent on the wall material composition and the infeed emulsion stability (Ramakrishnan et al., 2014). High EE values are generally related to fine and monodisperse emulsions stabilized with emulsifiers that are also able to maintain the integrity of the O/W interface during spray-drying (e.g., preventing oil droplets coalescence during atomization). Therefore, although the droplet size distribution of the parent emulsions before drying was similar for the different samples (D[4,3] = 0.451 ± 0.01 – 0.558 ± 0.007 μm) (Fig. 3), our results show that WPCH stabilized the oil droplets more efficiently during processing allowing a better entrapment of the oil within the carbohydrate wall matrix. In this regard, a recent study has shown that WPI alone prevented oil droplets coalescence during spray-drying more efficiently than WPI and low molecular weight emulsifiers combinations (e.g., WPI/Citrem) due to differences in the viscoelastic behavior of the interfacial layer (Taboada et al., 2021). High viscoelasticity of the interfacial layer is related to high molecular interactions emulsifier-oil and emulsifier-emulsifier, resulting in robust interfaces capable of preventing coalescence when the oil droplets come into close contact during atomization and drying (Taboada et al., 2021). Furthermore, it has been demonstrated that protein hydrolysis to a moderate degree of hydrolysis (DH; DH ≤ 10) results in peptides with enhanced emulsifying activity (Liceaga & Hall, 2018), which could increase the interfacial stability during processing to a higher extent. The magnitude of the complex dilatational modulus of the WPCH-based interfacial layer (E = 18.5 ± 0.9 mN/m) confirms its

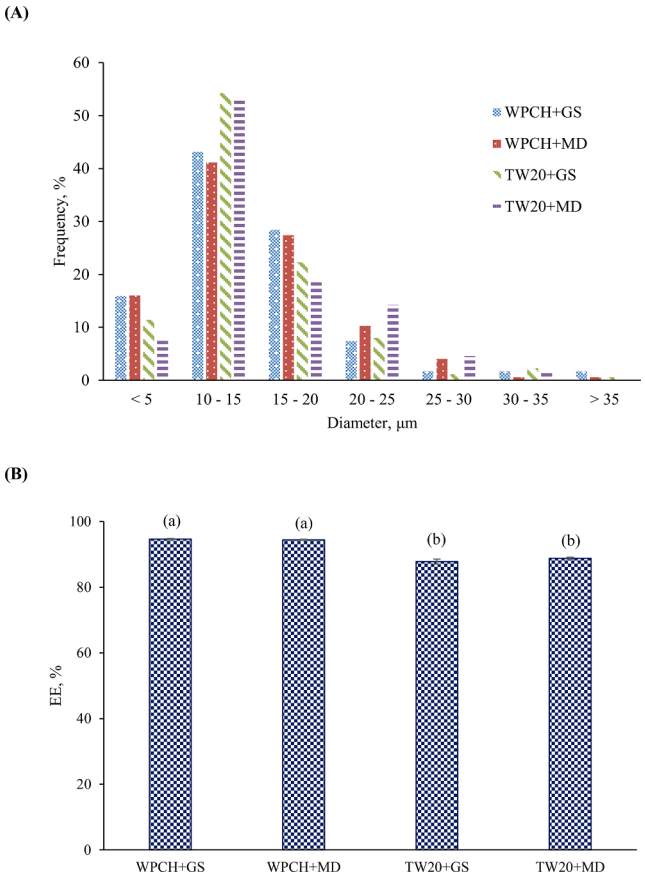

Fig. 2. Particle size distribution **(A)** and encapsulation efficiency (EE) **(B)** of the spray-dried microcapsules loaded with fish oil. Samples followed by a letter, a-b, indicates statistical differences ($p \leq 0.05$) between systems.

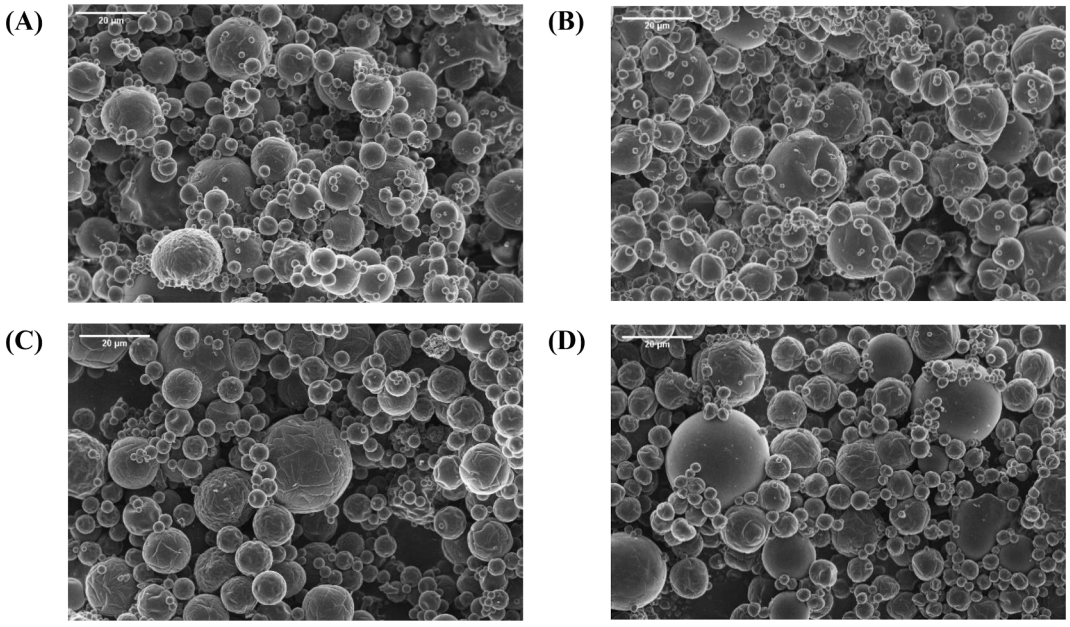

Fig. 1. SEM images of the fish oil-loaded microcapsules produced by spray-drying: WPCH + GS **(A)**, WPCH + MD **(B)**, TW20 + GS **(C)**, TW20 + MD **(D)**. Scale bar: 20 μm.

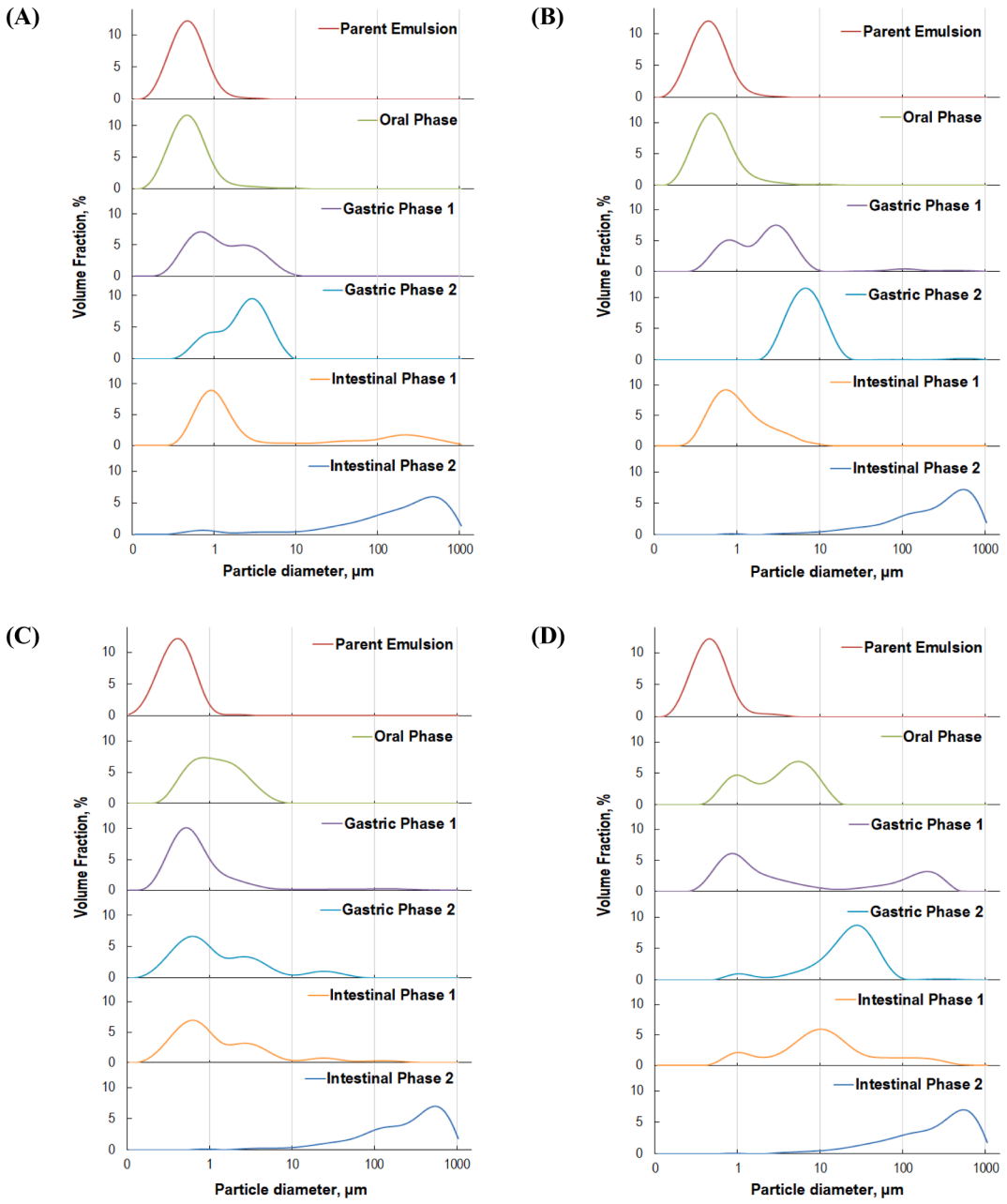

Fig. 3. Droplet size distribution of emulsions before (parent emulsion) and during *in vitro* digestion of samples: WPCH + GS **(A)**, WPCH + MD **(B)**, TW20 + GS **(C)**, TW20 + MD **(D)**. Gastric phase 1 and Intestinal phase 1 represent the droplet size distribution of oil droplets before adding the respective enzymes of the phase and Gastric phase 2 and Intestinal phase 2 represent the droplet size distribution of oil droplets at the end of each phase.

high viscoelastic behavior, with a predominant elastic behavior (interfacial elasticity: εd = 18.4.1 ± 1.0 mN/m, when measured at a frequency of 0.1 Hz, amplitude of deformation 5% and pH 8 for a concentration of WPCH of 0.1 mg/mL), as reported in our previous work (Ruiz-Álvarez et al., 2022).

3.2. *In vitro digestion*

The influence of the encapsulating agent (i.e., GS or MD) and the emulsifier (i.e., WPCH or TW20) used to produce the fish oil-loaded microcapsules on lipid bioaccessibility was investigated by measuring the rate and extent of lipolysis at the intestinal phase of the *in vitro* digestion. Previously, due to the water-soluble nature of the encapsulating agents used in this study, the fate of the microcapsules within the different stages of GIT was monitored by measuring the main emulsion stability indicators (e.g., droplet size distribution, charge of the interfacial layer, and microstructure).

3.2.1. *Oral phase*

After the oral phase of *in vitro* digestion, the droplet size of all the reconstituted emulsions increased with respect to the parent emulsions before drying (D[4,3] = 0.66 ± 0.01 – 4.24 ± 0.11 μm) (Fig. 3). WPCH-based systems showed a monomodal droplet size distribution and a similar droplet size that the respective parent emulsions, regardless of the encapsulating agent (D[4,3] = 0.66 ± 0.01 – 0.75 ± 0.01 μm) (Fig. 3A,B). However, the systems stabilized with TW20 showed both, wider and bimodal droplet size distributions and larger oil droplet size (D[4,3] = 1.54 ± 0.01 μm for sample TW20-GS and D[4,3] = 4.24 ± 0.11 μm for sample TW20-MD) (Fig. 3C,D). These results are consistent with the EE values reported for the microcapsules (Fig. 2B) since those

containing WPCH as an emulsifier showed the lowest content of non-encapsulated oil, hence less oil was available to coalesce after the dispersion of the microcapsules in the SSF. The latter was also confirmed by confocal microscopy images, where smaller oil droplets could be observed for the samples containing WPCH when compared to those produced with TW20 (Fig. 4A). Confocal microscopy images also showed differences in the oil droplets distribution within the sample depending on the encapsulating agent used in the formulation (Fig. 4A). Whilst for GS-containing systems the oil droplets were evenly distributed throughout the aqueous phase, droplets aggregation in the form of flocs were observed when MD was used as the encapsulating agent (Fig. 4A). This could be attributed to MD-induced depletion flocculation as a result of the different dextrose equivalence (DE) of the carbohydrates (DE21 for MD and DE38 for GS). Due to the lack of surface-active properties of the encapsulating biopolymers (i.e., GS or MD), these remained unabsorbed within the aqueous phase of the reconstituted emulsions. At the same free (bio)polymer concentration, depletion flocculation has been reported to be more strongly induced by molecules of higher molecular weight (Asakura & Oosawa, 1958), hence higher polymerization degree. This is the case of MD (DE21) over GS (DE38) since decreasing the DE of the carbohydrate leads to larger oligosaccharides of higher molecular weight. Furthermore, it could be observed that MD-induced depletion flocculation promoted coalescence of oil droplets to a higher extent for sample TW20 + MD compared to sample TW20 + GS, despite the SF content was similar for both microcapsules (12.1 ± 0.3% and 12.3 ± 0.8%, respectively). This was confirmed by the droplet size distribution of sample TW20 + MD, where a population of relatively large droplets could be noted (Fig. 3D). Interestingly, in the case of sample WPCH + MD, although flocs were formed, our results show that the integrity of the interfacial layer was retained avoiding droplets coalescence (Fig. 4A). The droplet size distribution of the aforementioned sample (Fig. 3B) also indicates that the MD-induced attractive forces were sufficiently low to be disrupted by the stirring conditions of the equipment used to do the measurements, as previously reported by other authors (Chang & McClements, 2016).

Fig. 5 shows that the interfacial layer coating the oil droplets after the oral phase of *in vitro* digestion was negatively charged for all the systems despite the different nature of the emulsifiers. TW20 is a non-ionic surfactant, and although no charge should be expected, it has been reported that oil droplets coated by Tweens are negatively charged

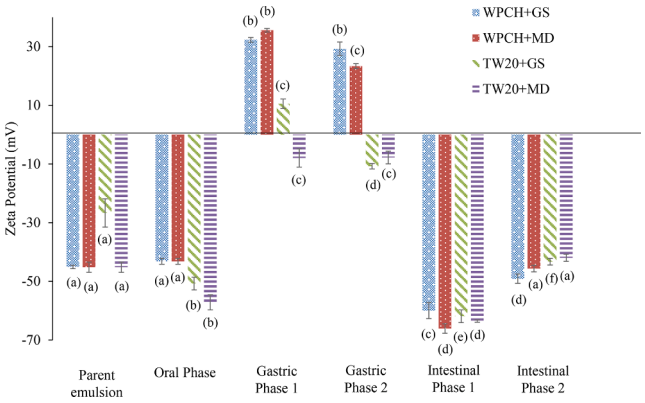

Fig. 5. ζ-potential of emulsions before (parent emulsion) and during *in vitro* digestion of samples. Gastric phase 1 and Intestinal phase 1 represent the ζ-potential of emulsions before adding the respective enzymes of the phase and Gastric phase 2 and Intestinal phase 2 represent ζ-potential of emulsions at the end of each phase. Samples followed by a letter, a-d, indicates statistical differences ($p \leq 0.05$) between the different stages of the GIT.

at neutral pH (Chang & McClements, 2016; Infantes-Garcia et al., 2021; Yang Li et al., 2020; Mun et al., 2007). The latter has been attributed either to the presence of impurities coming from the surfactant and/or the oil (i.e., free fatty acids), or due to the preferential adsorption of OH^- species from water. On the other hand, the negative ζ-potential values of the WPCH-stabilized systems were expected since the pH of the SSF (pH 7) is above the WPCH isoelectric point (pI = 4.06) (Ruiz-Álvarez et al., 2022). It should be noted that the magnitude of the electrical charge of the systems stabilized with WPCH did not significantly change with respect to the parent emulsions before drying ($p > 0.05$) (Fig. 5). Changes in the interfacial charge of oil droplets are related to changes in the O/W interface electrostatic interactions which further affect the overall emulsion stability (Infantes-Garcia et al., 2021). Therefore, taken altogether, it can be concluded that drying and subsequent re-dispersion of the microcapsules in SSF did not modify the properties of the WPCH-based interfacial layer. This is in agreement with our recent work reporting that spray-drying does not affect the secondary structure of WPCH peptides adsorbed at the O/W interface (Rahmani-Manglano

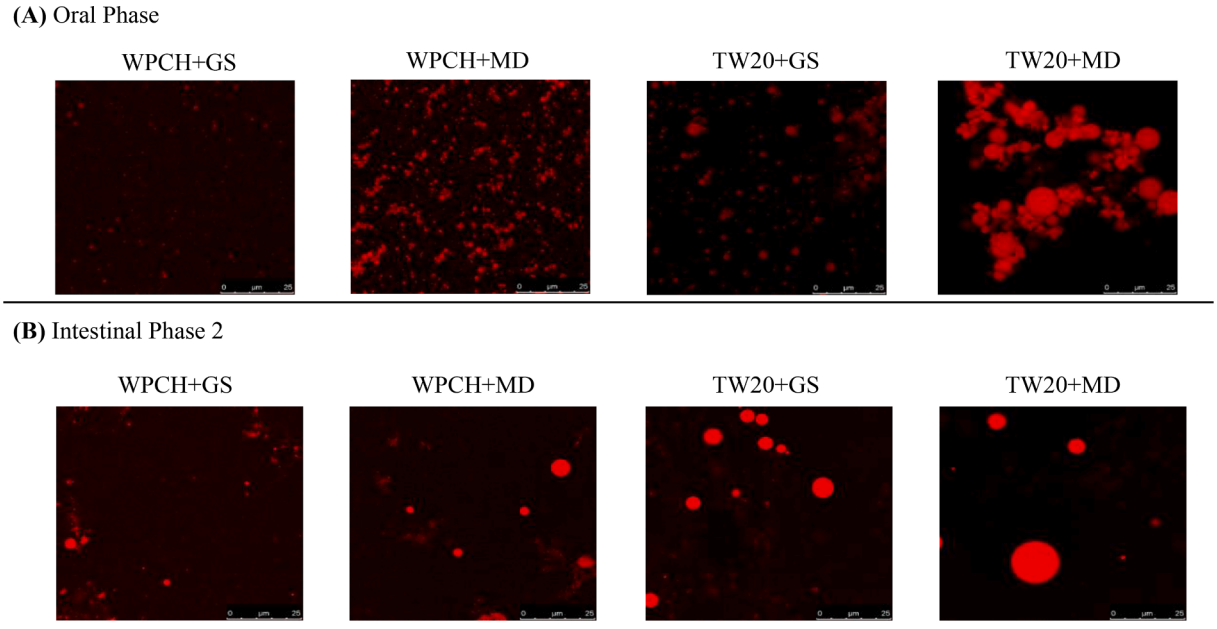

Fig. 4. Confocal microscopy images of the microstructure of the emulsions at the start (oral phase) (**A**), and at the end (after intestinal phase) (**B**) of the *in vitro* digestion process. Scale bar 25 μm.

et al., 2022).

3.2.2. Gastric phase

At the initial stage of the gastric phase of *in vitro* digestion (Gastric phase 1) the samples were adjusted to the gastric conditions (SGF, pH 3) but the enzyme was not added. As expected, passing through the WPCH isoelectric point (pI) altered the charge of the peptides' interfacial layer and the ζ-potential switched from negative to positive values (Fig. 5). The magnitude of the electrical charge was slightly reduced for both WPCH-based systems (from −43 mV to ca. 33 mV), which could be attributed to the electrostatic screening effect of the SGF (Chang & McClements, 2016). Changes in the medium pH and ionic strength have been reported to induce droplet aggregation in protein-stabilized emulsions (Chang & McClements, 2016; Singh & Ye, 2013), thus explaining the appearance of a population of large droplets on the droplet size distributions of the WPCH-containing emulsions (Fig. 3A,B). On the contrary, the ζ-potential absolute values of the TW20-based samples decreased significantly from ca. 51 – 57 mV to 8–10 mV (Fig. 5). The latter could be attributed to the presence of less negatively-charged ions in the continuous phase at the acidic conditions as well as to the electrostatic screening effect. Regarding the oil droplet size, this drastically increased for sample TW20 + MD, as shown in the oil droplet size distribution (Fig. 3D) suggesting further coalescence of the already coalesced oil droplets, which was not observed for sample TW20 + GS.

After the addition of the enzyme, and at the end of the simulated gastric phase of *in vitro* digestion (Gastric phase 2), the oil droplets surface net charge of TW20-based systems remained unvaried although TW20 + GS sample switched from positive to negative ζ-potential values. This could be attributed to the adsorption of negatively-charged pepsin molecules onto the surface of the positively-charged oil droplets at the acidic conditions of the simulated gastric phase due to the low isoelectric point of pepsin (pI = 1) (Andreeva & James, 1991). On the contrary, the electrical charge of the oil droplets coated by WPCH slightly decreased (Fig. 5). These results are in line with previous studies which showed that the surface charge of protein-stabilized emulsions decreases due to protein hydrolysis of the interfacial layer by pepsin (Singh & Ye, 2013). Proteolysis of whey proteins to a DH over 10% decrease their emulsifying properties (Padial-Domínguez et al., 2020b) since smaller peptides adsorbed at the O/W interface are unable to prevent droplet coalescence due to insufficient electrostatic and steric repulsions, as confirmed in Fig. 3A,B. Conversely, the results found for the TW20-based systems contrast with previous studies on the stability of Tween-stabilized emulsions under simulated gastric conditions (Chang & McClements, 2016; Infantes-Garcia et al., 2021; Yang Li et al., 2020). These authors reported that tweens, due to their non-ionic nature, efficiently stabilized the oil droplets due to steric repulsions irrespective of the medium pH. Therefore, little changes in the droplet size and on the droplets' aggregation state were observed after simulated gastric digestion (with respect to the emulsion at the begging of the gastric phase of each study) (Chang & McClements, 2016; Infantes-Garcia et al., 2021; Yang Li et al., 2020).

However, our results show that after the gastric phase of *in vitro* digestion the droplet size and droplet size distribution significantly changed (Fig. 3C,D). It is worth noting that the aforementioned studies did not subject the emulsions to spray-drying which may be indicative that the TW20-based interfacial layer integrity was not retained after processing.

3.2.3. Intestinal phase

Again, at the initial stage of the intestinal phase of *in vitro* digestion (Intestinal phase 1), the samples were adjusted to the intestinal conditions (SIF, bile extract, pH 7) but the enzymes were not added. At pH 7 and in the presence of bile extract, the ζ-potential values for all samples were highly negative and significantly different from that of the reconstituted emulsions after the oral phase of *in vitro* digestion ($p < 0.05$) (Fig. 5). Bile salts are amphiphilic molecules able to: i) emulsify bulk lipids entering the small intestine and ii) partially or totally displace the original emulsifier from the surface of already emulsified oil droplets (Maldonado-Valderrama et al., 2011). Bile salts adsorption upon the O/W interface is the crucial step of lipid digestion since the key role of these surface-active molecules is to promote lipolytic enzymes adsorption at the surface of oil droplets to initiate lipid hydrolysis (Bellesi & Pilosof, 2021). An increase in the negative charge of oil droplets under the simulated intestinal conditions (in the absence of enzymes) has been attributed to the presence of bile salts which could either adsorb upon the O/W interface together with the original emulsifier, partially or totally displace the original emulsifier or adsorb to the surface of the original emulsifier (Mun et al., 2007; Sarkar et al., 2016). Nonetheless, due to the nature of the emulsifiers used in this study, the decrease observed on the surface charge of the oil droplets is more likely to occur due to partial displacement of WPCH or TW20 originally adsorbed at the O/W interface (Maldonado-Valderrama et al., 2011).

The presence of bile extract in SIF also influenced the droplet size distribution of the samples in the absence of enzymes. As shown in Fig. 3, the presence of bile salts appears to exert a re-emulsifying effect for the samples studied, although it was more pronounced for WPCH-containing systems. TW20 have been reported to adsorb strongly to the surface of oil droplets hindering bile salts adsorption (Salvia-Trujillo et al., 2021), which could explain the droplet size results obtained. Whilst WPCH-based systems showed a mostly monomodal droplet size distribution notably different from that at the end of the gastric phase of *in vitro* digestion (Fig. 3A,B), TW20-based emulsions showed trimodal oil droplet size distributions similar to that at the end of the gastric phase (Fig. 3C,D). It should also be noted that the systems containing WPCH as emulsifier showed a large portion of small oil droplets at the beginning of the intestinal phase of *in vitro* digestion (main peak centered in ca. 0.7 – 0.9 μm) (Fig. 3A,B), confirming that bile salts displaced WPCH from the O/W interface leading to re-emulsification more efficiently than TW20 samples. These results contrast with other studies which reported that the oil droplet size of all the emulsions investigated increased after setting the samples to the simulated intestinal conditions in absence of enzymes regardless of the nature of the originally adsorbed emulsifier (Chang & McClements, 2016).

Lipid digestion is an interfacial process since lipase must adsorb onto the surface of the oil droplets to catalyze lipid hydrolysis. Therefore, the droplets' size and the droplets' aggregation state are important factors that have a high impact on omega-3 PUFAs bioaccessibility, especially at the beginning of the intestinal phase of digestion (McClements, 2018). Small oil droplets evenly distributed within the continuous phase are digested faster and more efficiently. This is related to a greater access of bile salts and lipase to the oil droplets surface and to the greater specific surface area available for lipase to be adsorbed (McClements, 2018; Salvia-Trujillo et al., 2021). Right after the addition of the enzymes (Intestinal phase 2), the rate of lipid digestion was monitored (Fig. 6A) and the total amount of FFA released after 2 h of incubation was calculated (Fig. 6B). Overall, the four types of microcapsules studied showed similar digestion profiles from which two regions could be clearly distinguished (Fig. 6A). During approximately the first 5 mins of incubation, a sharp increase in the release of the FFA could be observed for all the samples (region 1) followed by a sustained release until the end of the incubation time (region 2). The first region of the curve is related to a high lipolysis rate due to a fast adsorption of lipase onto the O/W surface and a rapid release of FFA to the continuous phase. Afterwards, the lipolysis rate tends to constant values because the products generated at the O/W interface (e.g., FFA, MAG) limit lipase adsorption and reduce enzyme activity (McClements, 2018). However, different trends on lipolysis rate and extent could be observed depending on the emulsifier used in the formulation of the fish oil-loaded microcapsules. The initial rate of FFA release (Fig. 6A) and the extent of lipolysis (Fig. 6B) of WPCH-based systems was higher than for those using TW20 as emulsifier. These results are in line with other studies which also reported lower lipid digestion on systems stabilized with TW20 over

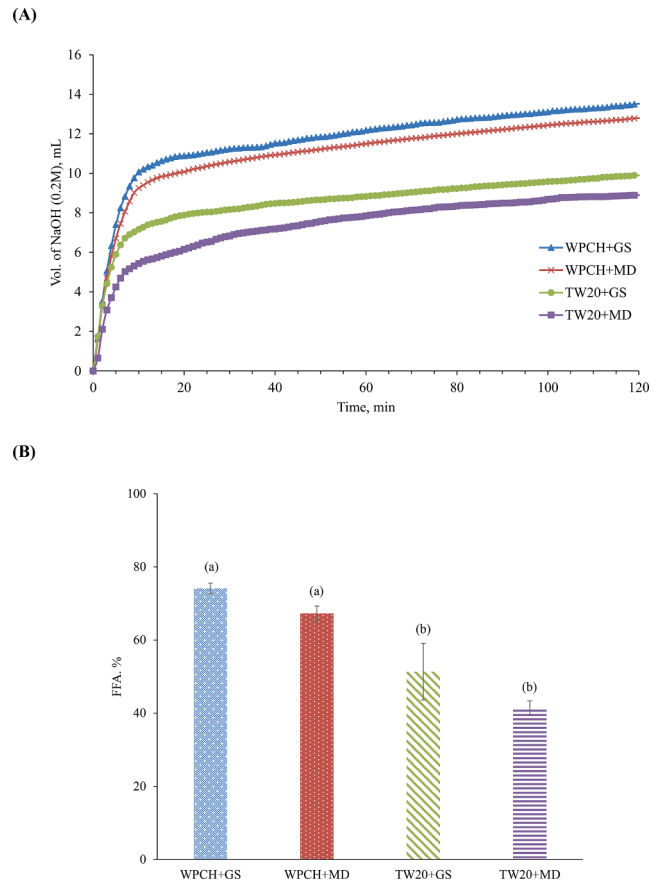

Fig. 6. Volume of NaOH (0.2 M) added during the intestinal phase of the *in vitro* digestion **(A)** and percentage of Free Fatty Acids (FFAs) released during the intestinal phase of the *in vitro* digestion measured using the pH-stat method **(B)**. Samples followed by a letter, a-b, indicates statistical differences ($p \leq 0.05$) between systems.

protein-based interfacial layers (Yang Li et al., 2020; Mun et al., 2007). This small-molecular weight emulsifier has been described to limit lipolysis because of its higher surface-activity compared to lipase which limits enzyme-substrate binding and subsequent reaction (Yang Li et al., 2020; Mun et al., 2007). However, the lower lipid digestion obtained for these samples cannot only be attributed to TW20 surface-activity. The oil droplets distribution within the continuous phase of TW20-containing samples compared to WPCH-stabilized systems at the beginning of the intestinal phase (Fig. 3) may have lowered lipolysis to a higher extent due to a reduction in the specific surface area available for lipase to adsorb in TW20-based samples as a consequence of oil droplets coalescence. Furthermore, although at the end of the simulated intestinal phase of digestion the droplet size and droplet size distribution were fairly similar among the samples (D[4,3] = 289.3 ± 39.3 – 342.0 ± 11.8 μm) (Fig. 3), confocal microscopy images (Fig. 4B) showed larger oil droplets for the systems containing TW20, most likely due to their lower lipid digestion. Conversely, the smaller oil droplets observed for WPCH-containing systems (Fig. 4B) may be attributed to the higher conversion of the TAG to FFA and MAG (Chang & McClements, 2016), thus confirming the higher lipolysis extent reported for the aforementioned samples (Fig. 6B). After the intestinal phase of *in vitro* digestion, all the samples showed negative surface charge (Fig. 5) which could be attributed to the presence of undigested protein aggregates or undigested lipid droplets (Chang & McClements, 2016).

By last, it is also worth mentioning that, although not significantly ($p > 0.05$), the encapsulating agent also seems to affect the overall lipolysis (Fig. 6B). Irrespective of the emulsifier used, the systems containing GS as encapsulating agent showed a slightly higher lipolysis rate (Fig. 6A) and a higher percentage of FFA released (Fig. 6B) at the end of the intestinal phase of *in vitro* digestion when compared to MD-containing samples. This could be attributed to the lower viscosity of the continuous phase in presence of GS compared to MD as a result of the different DE of the carbohydrates (Rahmani-Manglano et al., 2020b). The higher viscosity of the aqueous phase in presence of MD may difficult the diffusion of GIT components (e.g., digestive enzymes) through the medium to the oil droplets' surface, as well as the diffusion of lipolysis products (e.g., FFA, MAG) from the oil droplets' surface to the medium (Chang & McClements, 2016).

4. Conclusions

The emulsifier used in the feed emulsion formulation for spray-drying had a major impact on the bioaccessibility of micro-encapsulated fish oil. WPCH prevented oil droplet coalescence during processing and after re-dispersion of the microcapsules in the simulated fluids of the GIT, contrary to TW20. This resulted in a higher specific surface area of the WPCH-stabilized systems for adsorption of bile salts and lipase, hence a higher lipolysis rate and extent was obtained for the aforementioned samples. Furthermore, although not significantly, the encapsulating agent also affected lipid digestion. Irrespective of the emulsifier used, GS-containing systems showed higher percentages of FFA released after the intestinal phase of *in vitro* digestion. The latter has been attributed to the different viscosities of the digest in presence of GS or MD. Overall, our results show the high bioaccessibility of fish oil-loaded microcapsules produced by spray-drying when using WPCH as emulsifier.

CRediT authorship contribution statement

Nor E. Rahmani-Manglano: Methodology, Formal analysis, Writing – original draft. **Manuel Tirado-Delgado:** Methodology, Formal analysis, Writing – original draft. **Pedro J. García-Moreno:** Conceptualization, Methodology, Supervision, Writing – review & editing. **Antonio Guadix:** Supervision, Writing – review & editing. **Emilia M. Guadix:** Supervision, Writing – review & editing, Funding acquisition.

Declaration of Competing Interest

The authors declare that they have no known competing financial interests or personal relationships that could have appeared to influence the work reported in this paper.

Acknowledgements

This work was supported by the I + D + i projects CTQ2017-87076-R and PID2020-114137RB-I00 funded by MCIN/AEI/10.13039/501100011033/. N. E. Rahmani-Manglano acknowledges an FPI grant PRE2018-084861 funded by MCIN/AEI/10.13039/501100011033. Funding for open access charge: Universidad de Granada / CBUA.

References

Acevedo-Fani, A., Guo, Q., Nasef, N., & Singh, H. (2021). Aspects of food structure in digestion and bioavailability of LCn-3PUFA-rich lipids. In P. J. García-Moreno, C. Jacobsen, A.-.-D.-M. Sørensen, & B. Yesiltas (Eds.), *Omega-3 Delivery Systems* (pp. 427–448). Academic Press. https://doi.org/10.1016/b978-0-12-821391-9.00003-x.

Andreeva, N. S., & James, M. N. G. (1991). Why does pepsin have a negative charge at very low ph? an analysis of conserved charged residues in aspartic proteinases. In *Structure and Function of the Aspartic Proteinases. Advances in Experimental Medicine and Biology* (pp. 39–45). https://doi.org/10.1007/978-1-4684-6012-4_4

Asakura, S., & Oosawa, F. (1958). Interaction between Particles Suspended in Solutions of Macromolecules. *Journal of Polymer Science, XXXIII*, 183–192.

Bellesi, F. A., & Pilosof, A. M. R. (2021). Potential implications of food proteins-bile salts interactions. *Food Hydrocolloids, 118*(106766). https://doi.org/10.1016/j.foodhyd.2021.106766

Brodkorb, A., Egger, L., Alminger, M., Alvito, P., Assunção, R., Ballance, S., … Recio, I. (2019). INFOGEST static in vitro simulation of gastrointestinal food digestion. *Nature Protocols, 14*(4), 991–1014. https://doi.org/10.1038/s41596-018-0119-1

Calder, P. C., & Yaqoob, P. (2009). Omega-3 polyunsaturated fatty acids and human health outcomes. *BioFactors, 35*(3), 266–272. https://doi.org/10.1002/biof.42

Champagne, C. P., & Fustier, P. (2007). Microencapsulation for the improved delivery of bioactive compounds into foods. *Current Opinion in Biotechnology, 18*(2), 184–190. https://doi.org/10.1016/j.copbio.2007.03.001

Chang, C., & Nickerson, M. T. (2018). Stability and in vitro release behaviour of encapsulated omega fatty acid-rich oils in lentil protein isolate-based microcapsules. *International Journal of Food Sciences and Nutrition, 69*(1), 12–23. https://doi.org/10.1080/09637486.2017.1336513

Chang, Y., & McClements, D. J. (2016). Influence of emulsifier type on the in vitro digestion of fish oil-in-water emulsions in the presence of an anionic marine polysaccharide (fucoidan): Caseinate, whey protein, lecithin, or Tween 80. *Food Hydrocolloids, 61*, 92–101. https://doi.org/10.1016/j.foodhyd.2016.04.047

El-Messery, T. M., Altuntas, U., Altin, G., & Özçelik, B. (2020). The effect of spray-drying and freeze-drying on encapsulation efficiency, in vitro bioaccessibility and oxidative stability of krill oil nanoemulsion system. *Food Hydrocolloids, 106*(105890). https://doi.org/10.1016/j.foodhyd.2020.105890

Encina, C., Vergara, C., Giménez, B., Oyarzún-Ampuero, F., & Robert, P. (2016). Conventional spray-drying and future trends for the microencapsulation of fish oil. *Trends in Food Science and Technology, 56*, 46–60. https://doi.org/10.1016/j.tifs.2016.07.014

Favé, G., Coste, T. C., & Armand, M. (2004). Physicochemical properties of lipids: New strategies to manage fatty acid bioavailability. *Cellular and Molecular Biology (Noisy-Le-Grand, France), 50*(7), 815–831. https://doi.org/10.1170/T575

Infantes-Garcia, M. R., Verkempinck, S. H. E., Gonzalez-Fuentes, P. G., Hendrickx, M. E., & Grauwet, T. (2021). Lipolysis products formation during in vitro gastric digestion is affected by the emulsion interfacial composition. *Food Hydrocolloids, 110* (106163). https://doi.org/10.1016/j.foodhyd.2020.106163

Jacobsen, C., Nielsen, N. S., Horn, F. F., & Sørensen, A. D. M. (2013). Food enrichment with omega-3 fatty acids. In *Food Enrichment with Omega-3 Fatty Acids*. https://doi.org/10.1533/9780857098863

Li, Y., & Mcclements, D. J. (2010). New mathematical model for interpreting ph-stat digestion profiles: Impact of lipid droplet characteristics on in vitro digestibility. *Journal of Agricultural and Food Chemistry, 58*(13), 8085–8092. https://doi.org/10.1021/jf101325m

Li, Y., Li, M., Qi, Y., Zheng, L., Wu, C., Wang, Z., & Teng, F. (2020). Preparation and digestibility of fish oil nanoemulsions stabilized by soybean protein isolate-phosphatidylcholine. *Food Hydrocolloids, 100*(105310). https://doi.org/10.1016/j.foodhyd.2019.105310

Liceaga, A. M., & Hall, F. (2018). Nutritional, functional and bioactive protein hydrolysates. In *Encyclopedia of Food Chemistry*. Elsevier. https://doi.org/10.1016/B978-0-08-100596-5.21776-9.

Maldonado-Valderrama, J., Wilde, P., MacIerzanka, A., & MacKie, A. (2011). The role of bile salts in digestion. *Advances in Colloid and Interface Science, 165*(1), 36–46. https://doi.org/10.1016/j.cis.2010.12.002

Mat, D. J. L., Le Feunteun, S., Michon, C., & Souchon, I. (2016). In vitro digestion of foods using pH-stat and the INFOGEST protocol: Impact of matrix structure on digestion kinetics of macronutrients, proteins and lipids. *Food Research International, 88*, 226–233. https://doi.org/10.1016/j.foodres.2015.12.002

McClements, D. J. (2018). Enhanced delivery of lipophilic bioactives using emulsions: A review of major factors affecting vitamin, nutraceutical, and lipid bioaccessibility. *Food and Function, 9*(1), 22–41. https://doi.org/10.1039/c7fo01515a

Minekus, M., Alminger, M., Alvito, P., Ballance, S., Bohn, T., Bourlieu, C., … Brodkorb, A. (2014). A standardised static in vitro digestion method suitable for food-an international consensus. *Food and Function, 5*(6), 1113–1124. https://doi.org/10.1039/c3fo60702j

Moreau, H., Gargouri, Y., Lecat, D., Junien, J. L., & Verger, R. (1988). Purification, characterization and kinetic properties of the rabbit gastric lipase. *Biochimica et Biophysica Acta (BBA)/Lipids and Lipid. Metabolism, 960*(3), 286–293. https://doi.org/10.1016/0005-2760(88)90036-7

Mun, S., Decker, E. A., & McClements, D. J. (2007). Influence of emulsifier type on in vitro digestibility of lipid droplets by pancreatic lipase. *Food Research International, 40*(6), 770–781. https://doi.org/10.1016/j.foodres.2007.01.007

Padial-Domínguez, M., Espejo-Carpio, F. J., García-Moreno, P. J., Jacobsen, C., & Guadix, E. M. (2020). Protein derived emulsifiers with antioxidant activity for stabilization of omega-3 emulsions. *Food Chemistry, 329*(127148). https://doi.org/10.1016/j.foodchem.2020.127148

Padial-Domínguez, M., Espejo-Carpio, F. J., Pérez-Gálvez, R., Guadix, A., & Guadix, E. M. (2020). Optimization of the emulsifying properties of food protein hydrolysates for the production of fish oil-in-water emulsions. *Foods, 9*(5). https://doi.org/10.3390/foods9050636

Punia, S., Sandhu, K. S., Siroha, A. K., & Dhull, S. B. (2019). Omega 3-metabolism, absorption, bioavailability and health benefits–A review. *PharmaNutrition, 10*, Article 100162. https://doi.org/10.1016/j.phanu.2019.100162

Rahmani-Manglano, N. E., García-Moreno, P. J., Espejo-Carpio, F. J., Pérez-Gálvez, A. R., & Guadix-Escobar, E. M. (2020a). The Role of Antioxidants and Encapsulation Processes in Omega-3 Stabilization. In M. A. Aboudzadeh (Ed.), *Emulsion-based Encapsulation of Antioxidants. Food Bioactive Ingredients* (pp. 339–386). Cham: Springer. https://doi.org/10.1007/978-3-030-62052-3_10.

Rahmani-Manglano, N. E., González-Sánchez, I., García-Moreno, P. J., Espejo-Carpio, F. J., Jacobsen, C., & Guadix, E. M. (2020). Development of fish oil-loaded microcapsules containing whey protein hydrolysate as film-forming material for fortification of low-fat mayonnaise. *Foods, 9*(5). https://doi.org/10.3390/foods9050545

Rahmani-Manglano, N. E., Jones, N. C., Hoffmann, S. V., Guadix, E. M., Pérez-Gálvez, R., Guadix, A., & García-Moreno, P. J. (2022). Structure of whey protein hydrolysate used as emulsifier in wet and dried oil delivery systems: Effect of pH and drying processing. *Food Chemistry, 390*. https://doi.org/10.1016/j.foodchem.2022.133169

Ramakrishnan, S., Ferrando, M., Aceña-Muñoz, L., Mestres, M., De Lamo-Castellví, S., & Güell, C. (2014). Influence of Emulsification Technique and Wall Composition on Physicochemical Properties and Oxidative Stability of Fish Oil Microcapsules Produced by Spray Drying. *Food and Bioprocess Technology, 7*(7), 1959–1972. https://doi.org/10.1007/s11947-013-1187-4

Ruiz-Álvarez, J. M., del Castillo-Santaella, T., Maldonado-Valderrama, J., Guadix, A., Guadix, E. M., & García-Moreno, P. J. (2022). pH influences the interfacial properties of blue whiting (M. poutassou) and whey protein hydrolysates determining the physical stability of fish oil-in-water emulsions. *Food Hydrocolloids, 122*(107075). https://doi.org/10.1016/j.foodhyd.2021.107075

Salvia-Trujillo, L., McClements, D. J., & Martín-Belloso, O. (2021). Nanoemulsion design for the delivery of omega-3 fatty acids: Formation, oxidative stability, and digestibility. In P. J. García-Moreno, C. Jacobsen, A.-.-D.-M. Sørensen, & B. Yesiltas (Eds.), *Omega-3 Delivery Systems* (pp. 295–319). Academic Press. https://doi.org/10.1016/b978-0-12-821391-9.00016-8.

Sánchez, C. A. O., Zavaleta, E. B., García, G. R. U., Solano, G. L., & Díaz, M. P. R. (2021). Krill oil microencapsulation: Antioxidant activity, astaxanthin retention, encapsulation efficiency, fatty acids profile, in vitro bioaccessibility and storage stability. *Lwt, 147*(April). https://doi.org/10.1016/j.lwt.2021.111476

Sarkar, A., Ye, A., & Singh, H. (2016). On the role of bile salts in the digestion of emulsified lipids. *Food Hydrocolloids, 60*, 77–84. https://doi.org/10.1016/j.foodhyd.2016.03.018

Shen, Z., Apriani, C., Weerakkody, R., Sanguansri, L., & Augustin, M. A. (2011). Food matrix effects on in vitro digestion of microencapsulated tuna oil powder. *Journal of Agricultural and Food Chemistry, 59*(15), 8442–8449. https://doi.org/10.1021/jf201494b

Singh, H., & Ye, A. (2013). Structural and biochemical factors affecting the digestion of protein-stabilized emulsions. *Current Opinion in Colloid and Interface Science, 18*(4), 360–370. https://doi.org/10.1016/j.cocis.2013.04.006

Solomando, J. C., Antequera, T., & Perez-Palacios, T. (2020). Lipid digestion products in meat derivatives enriched with fish oil microcapsules. *Journal of Functional Foods, 68*. https://doi.org/10.1016/j.jff.2020.103916

Solomando, J. C., Antequera, T., & Pérez-Palacios, T. (2020). Study on fish oil microcapsules as neat and added to meat model systems: Enrichment and bioaccesibility of EPA and DHA. *LWT, 120*(108946). https://doi.org/10.1016/j.lwt.2019.108946

Taboada, M. L., Heiden-Hecht, T., Brückner-Gühmann, M., Karbstein, H. P., Drusch, S., & Gaukel, V. (2021). Spray drying of emulsions: Influence of the emulsifier system on changes in oil droplet size during the drying step. *Journal of Food Processing and Preservation, 45*(9), 1–11. https://doi.org/10.1111/jfpp.15753

Yang, J., & Ciftci, O. N. (2020). In vitro bioaccessibility of fish oil-loaded hollow solid lipid micro- and nanoparticles. *Food and Function, 11*(10), 8637–8647. https://doi.org/10.1039/d0fo01591a

Zhu, Y., Peng, Y., Wen, J., & Quek, S. Y. (2021). A comparison of microfluidic-jet spray drying, two-fluid nozzle spray drying, and freeze-drying for co-encapsulating β-carotene, lutein, zeaxanthin, and fish oil. *Foods, 10*(7). https://doi.org/10.3390/foods10071522